# CrystEngComm

Accepted Manuscript






ROYAL SOCIETY OF CHEMISTRY

www.rsc.org/crystengcomm

*CrystEngComm*

ARTICLE

# Isoniazid cocrystallisation with dicarboxylic acids: vapochemical, mechanochemical and thermal methods

Received 00th January 20xx,
Accepted 00th January 20xx

DOI: 10.1039/x0xx00000x

www.rsc.org/

I. Sarceviča,[a†] A. Kons[a] and L. Orola[a]

Cocrystallisation with a series of related compounds allows for the exploration of trends and limitations set by structural differences between these compounds. In this work, we investigate how the length of a dicarboxylic acid influences the outcome of cocrystallisation with isoniazid. We have performed a systematic study on the mechanochemical, thermal and solvent vapour-assisted cocrystallisation of aliphatic dicarboxylic acids ($C_3$–$C_{10}$) with isoniazid. Our results demonstrate that the rate of mechanochemical and vapour-assisted cocrystallisation depends on acid chain length and shows alternation between odd- and even- chain acids. The results of thermal cocrystallisation showed that eutectic melting temperatures of isoniazid–dicarboxylic acid mixtures follow the same trend as do the melting points of dicarboxylic acids.

## Introduction

As a way to improve the characteristics of materials, cocrystal form has recently became of a large interest[1–4]. The possibility to tune the properties of compounds *via* cocrystallisation has been shown[2,3,5] and has been used to develop new materials for non-linear optics[6,7], semiconductors[8] and pharmaceutical applications[1–3]. Various methods based on crystallisation from solution[9–12] or from melt (thermal cocrystallisation)[11,13,14], mechanical treatment[15–18] etc. are used for cocrystal preparation. From these, the mechanochemical cocrystallisation is typically recognised to give the best results[11], moreover, liquid-assisted grinding is more efficient compared to neat grinding (no solvent used). In screening experiments that employ and compare different cocrystallisation methods, solvent–drop grinding has been shown to produce the largest number of cocrystals[11]. In addition, mechanochemistry allows inter-conversion between cocrystals[19] of different stoichiometry and polymorphism control[20,21]. Further benefits of the mechanochemical method include minimal use of solvent, high yields and easiness to perform[17].

The thermal cocrystallisation method is based on understanding that cocrystals can form from the eutectic melt. The presence of thermal effects (in the thermal analysis data) corresponding to eutectic melting and crystallisation implies formation of a cocrystal[13,22]. The thermal method is a fast method compared to crystallisation from solution. Alongside mechanochemistry, thermal cocrystallisation also usually gives good results in cocrystal screening[11,14] and can be efficiently used to identify systems that can form cocrystals.

Spontaneous cocrystallisation is also possible[23] and is usually facilitated by moisture[24,25]. Although the promotional effect of the vapour of water[24,25] or organic solvent[26,27] on cocrystallisation is known and has been investigated by several groups, little practical advantage of this knowledge has been gained until now. Perhaps the lack of appreciation for solvent vapour-assisted cocrystallisation as a cocrystal screening method stems from the difficulty in predicting whether it will be useful in the system of interest. Consequently, this method mostly has been neglected in systematic screenings and only individual cases of vapour-assisted cocrystallisation have been reported. Our results, however, imply that vapochemistry could be beneficial for cocrystallisation of small molecules. In order to evaluate the usability of the vapochemical approach in each system, it is important to understand the limitations set by the molecular parameters of cocrystal ingredients and by solvent properties. One of the possible limitations could be the size of molecules, as the movement of large molecules would be hampered.

There are several explanations available for the promotional effect of water vapour on cocrystal formation. In some cases, the adsorbed water has been shown to partially dissolve cocrystal ingredients, allowing cocrystallisation from a saturated solution[24,25]. In other examples water serves as a plasticizer and therefore promotes cocrystallisation[28]. Various solvents are expected to influence cocrystallisation differently in accordance with their properties. Therefore, solvent vapour-assisted cocrystallisation is also expected to offer polymorph control, similar to crystallization from different solvents[29].

[a] *Department of Chemistry, University of Latvia, Jelgavas street 1, Riga, Latvia, LV-1004*
† Inese.Sarcevica@lu.lv

Electronic Supplementary Information (ESI) available: PXRD pattern examples of mechanochemical and thermal cocrystallisation experiments, a list of physicochemical property parameters of solvents and crystal structure data (CCDC 1422395) of isoniazid–adipic acid cocrystal form II. See DOI: 10.1039/x0xx00000x

A commonly used set of cocrystal formers is the series of aliphatic dicarboxylic acids[30–33]. The choice of these dicarboxylic acids as cocrystal formers is advantageous in many aspects. They easily form cocrystals with hydrogen acceptor compounds; their crystal structures[34] and physicochemical properties[35–39] are described in the literature. In addition, dicarboxylic acids offer a set of related compounds with similar molecular structures, and therefore render the interpretation of results easier. Most physicochemical properties of dicarboxylic acids follow an interesting trend of alternation between odd- and even-chain acids. For example, the solubility[35,36] and saturated vapour pressure[37,38,40] of odd-chain acids are higher than for even-chain acids. The melting points[34] and vaporisation enthalpies[40] of odd-chain acids are lower, compared with those of even-chain acids. These trends are commonly explained by the twisted conformations of odd-chain acids in their crystal structures[34,37], leading to lower stability of these structures compared with crystal structures of even-chain acids. Interestingly, the cocrystals of dicarboxylic acids also often show the odd-even alternation effect in their physicochemical properties[30–33].

Here we report a series of experiments that demonstrate the vapour-assisted, thermal and mechanochemical cocrystallisation of an anti-tubercular drug isoniazid with aliphatic dicarboxylic acids ($C_3$–$C_{10}$) as cocrystal formers (Scheme 1). Isoniazid was chosen as a model compound for our experiments as it is known to form cocrystals with all $C_3$–$C_8$ dicarboxylic acids[41,42] and many other acidic compounds[41,43–53]. Organometallic complexes[54–58] and salts[59,60] with inorganic anions of isoniazid are also known. Our experiments reveal how the length of the acid and its physicochemical properties determine trends in cocrystal formation with isoniazid.

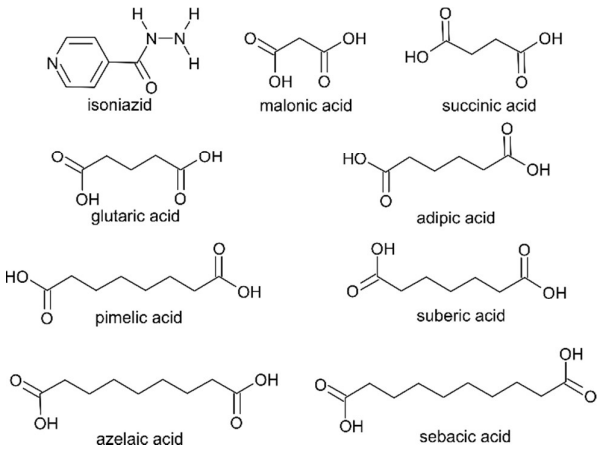


**Scheme 1**. Structural formulas of isoniazid and $C_3$-$C_{10}$ dicarboxylic acids.

## Results and discussion

It has been found previously[41,42] that isoniazid forms 1:1 cocrystals with odd-chain dicarboxylic acids and 2:1 cocrystals with even-chain dicarboxylic acids. An exception is the isoniazid–malonic acid cocrystal, which has the 2:1 stoichiometry, although malonic acid is an odd-chain dicarboxylic acid. In our mechanochemical, thermochemical and vapochemical cocrystallisation experiments, we used these known stoichiometries.

### Mechanochemical cocrystallisation

To investigate the effect of molecule size on the rate of mechanochemical cocrystal formation, milling experiments were performed for isoniazid and dicarboxylic acid ($C_3$–$C_{10}$) mixtures. The conversion (relative amount of cocrystal in a sample) was acquired by Rietveld analysis of the diffraction patterns of milling products. Inspection of PXRD patterns of milling products showed that they contain cocrystal phases with the known crystal structures[41] of isoniazid–dicarboxylic acid cocrystals, and these structures were used in Rietveld refinement. It should be noted that some peak broadening and minor background changes were observed in the powder X-ray diffraction (PXRD) patterns of milling products, implying a possible presence of amorphous phase. Results of the quantitative analysis should therefore not be seen as absolute values, but rather as an indication of the extent of cocrystallisation (the amount of the cocrystal relative to the amounts of crystalline isoniazid and acid). Examples of PXRD patterns of milling products are available in Figures S1–S8 in ESI.

Figure 1 presents cocrystallisation results for isoniazid and dicarboxylic acid milling experiments performed for 5 and 15 minutes under the same conditions. A comparison of the results shows that longer mechanical treatment returned a higher amount of cocrystal. In the case of isoniazid–glutaric acid sample, however, the conversion difference was small due to partial amorphisation and formation of an unidentified phase.

Cocrystallisation of isoniazid and malonic acid proceeded rapidly compared with other dicarboxylic acids, and almost complete conversion was achieved after 5 minutes of milling. We observed that isoniazid–malonic acid cocrystal starts to form already during sample preparation under laboratory conditions, and milling accelerates the reaction. Cocrystallisation with $C_4$–$C_7$ dicarboxylic acids proceeded considerably more slowly than cocrystallisation with malonic acid and the conversion after 5 minutes did not exceed 40% in any of these samples.

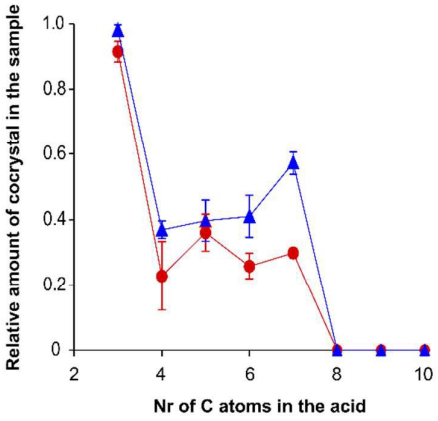


**Fig. 1** The relative amount of cocrystal in isoniazid and dicarboxylic acid milling (20 Hz; 5 (red) and 15 (blue) minutes) products as a function of acid chain length.

In order to evaluate the time necessary to achieve complete conversion, we performed experiments with extended milling time. These results showed that the conversion time for isoniazid–succinic acid cocrystal is approximately 200 minutes and the product contains pure cocrystal phase (Figure S2 in ESI). The co-milling of isoniazid and glutaric acid required approximately 150 minutes, and the product contained residue of isoniazid but not glutaric acid (Figure S3 in ESI). Significant amorphisation for this sample was also observed. The diffraction reflections corresponding to an unidentified phase observed during the initial stage of treatment later disappeared implying that this phase is possibly an intermediate. For the isoniazid–adipic acid sample, formation of two polymorphic forms of the cocrystal (I and II) was observed depending on the milling time (Figure S4 in ESI). Initially, the form I (the known polymorph of isoniazid – adipic acid cocrystal) was acquired but later it converted to a new polymorphic form II. This cocrystal also formed in milling experiments if the milling frequency was 30 Hz and the milling time exceeded 30 minutes. The isoniazid–adipic acid cocrystal polymorph II could also be prepared by pre-milling the 2:1 physical mixture of isoniazid and adipic acid and then keeping this mixture in the presence of water vapour. A comparison of the diffraction patterns simulated form crystal structures of both isoniazid–adipic acid polymorphs and cocrystal ingredients is shown in figure 2.

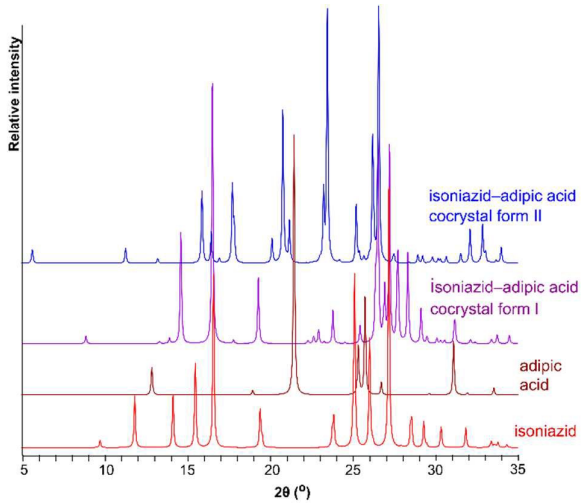


**Fig. 2** Comparison of simulated powder X-ray diffraction patterns of isoniazid, adipic acid, isoniazid–adipic acid cocrystal form I and isoniazid–adipic acid cocrystal form II.

Traces of isoniazid were observed in the powder X-ray diffraction patterns of the product even after 260 minutes of milling, but the presence of the adipic acid was not detected. The formation of isoniazid–pimelic acid cocrystal required approximately an hour; the final product contained traces of unreacted isoniazid (Figure S5 in ESI).

The cocrystallisation of longer-chain acids (suberic acid, azelaic acid, sebacic acid) was not achieved by milling at 20 Hz for up to 15 minutes. However, after an hour of co-milling isoniazid with suberic acid, formation of the cocrystal took place (Figure S6 in ESI). Even longer milling, up to 200 minutes, allowed obtaining the cocrystal with only traces of isoniazid (and again – no suberic acid). The isoniazid–azelaic acid cocrystal in mechanochemical experiments was not obtained even after 300 minutes of milling (Figure S7 in ESI). In the mixture of isoniazid and sebacic acid, cocrystal formation was observed after 200 minutes of milling but it proceeded very slowly and even 300 minutes of mechanical treatment was not sufficient to achieve complete conversion to cocrystal (Figure S8 in ESI).

Since amorphisation to some degree was observed for most of the samples, additional experiments were executed to evaluate the changes related to the crystallinity of the acids during milling. The results of these experiments showed increase in the diffraction peak width with increasing acid chain length. The peak broadening can be related to partial amorphisation of the acid as well as the reduction of particle size.

The differences in the mechanochemical reaction rate between acids can be related to several factors including the stability of the lattice of the acid, mobility of molecules and partial amorphisation of acids during milling. An alternation between formation rates of isoniazid cocrystals with odd- and even-chain acids was observed with the malonic, glutaric and pimelic acid cocrystals forming faster, compared with cocrystals with adjacent even-chain acids. Similar odd-even alternation effects have been observed for many physicochemical properties (solubility, melting points, etc.) of

dicarboxylic acids[35,36] implying that the stability of even-chain acid crystal structures is higher than that of odd-chain dicarboxylic acid crystal structures. The disintegration of the less stable odd-chain diacid crystal structures therefore requires less energy leading to an easier cocrystallisation.

The outcome of mechanochemical cocrystallisation also depends on mass transfer processes[61] and the rate of cocrystal formation is therefore affected by the ability of molecules to move. Small molecules, which generally tend to be more mobile, cocrystallise faster than larger molecules. The effect of the size of molecules is demonstrated by the isoniazid cocrystals with suberic and sebacic acid that required much longer time to form compared with other cocrystals with shorter acids.

Interestingly, the amorphisation during mechanochemical milling does not correlate with the amorphisation of pure acids (Figures S9-S16 in ESI). Considerable peak broadening and background changes were observed for isoniazid–glutaric acid and isoniazid–succinic acid samples although these acids did not show high amorphisation when milled separately. The amorphisation of these samples could therefore be related to partial eutectic melting during the milling process.

**Thermal cocrystallisation**

Crystallisation from eutectic melt is another popular way of preparing cocrystals, and it is often used as a fast and efficient screening method[13,22]. The odd-even alternation between values of melting points of dicarboxylic acids[34] and their cocrystals[30,33] encouraged us to study the relation between the length of the dicarboxylic acid and the eutectic temperatures in mixtures with isoniazid. The eutectic temperatures were acquired from differential thermal analysis (DTA) of physical mixtures of isoniazid and dicarboxylic acids and are shown in Figure 3 along with the melting points of pure diacids and their cocrystals with isoniazid. The melting points of cocrystals were also taken from DTA results and corresponded to the recrystallisation product of the eutectic mixture.

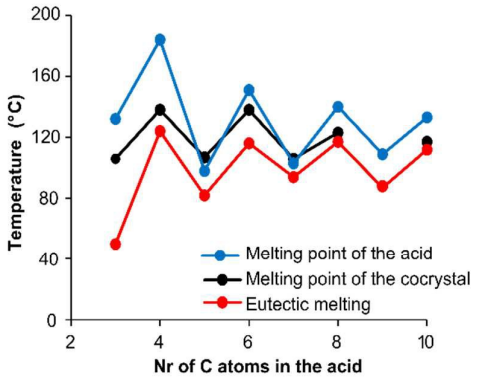


**Fig. 3** Melting points of pure dicarboxylic acids, their cocrystals with isoniazid and the eutectic temperatures of isoniazid–dicarboxylic acid physical mixtures.

The eutectic temperatures of isoniazid–dicarboxylic acid mixtures show similar pattern to melting points of pure acids. The eutectic temperatures and acid melting points are higher for isoniazid mixtures with even-chain acids than for odd-chain acids. In the DTA curve of the isoniazid–azelaic acid 1:1 mixture, only one peak was observed implying that recrystallisation from melt had not taken place.

The values of cocrystal melting points are between the values of eutectic temperatures and the melting points of acids, with the exceptions of glutaric acid and pimelic acid. The melting points of isoniazid–glutaric acid cocrystal and isoniazid–pimelic acid cocrystal are slightly higher compared to melting points of pure acids. Interestingly, the DTA curve of isoniazid–malonic acid sample did not show a distinct endothermic effect corresponding to eutectic melting of the cocrystal. A broad exothermic effect, thought to be the recrystallization of the cocrystal occurred at 65 °C.

Thermal analyses do not provide information on the structure of cocrystallisation products; therefore, we used variable temperature powder X-ray diffraction experiments (VT-PXRD) to obtain more information on the products of thermal cocrystallisation. The VT-PXRD analysis implied that the isoniazid cocrystals of malonic, succinic, glutaric, pimelic, suberic and sebacic acids obtained using the thermal method were the same as reported in the literature[41] and as obtained mechanochemically, although the samples of isoniazid–malonic acid and isoniazid–glutaric acid cocrystals also contained an unidentified phase (Figures S17–S23 in ESI). The thermal cocrystallisation products of odd-chain acids (malonic acid, glutaric acid, pimelic acid) also contained residues of isoniazid as the dicarboxylic acid had vaporised at elevated temperature. The formation of isoniazid–azelaic acid cocrystal *via* eutectic melting was not observed.

The isoniazid–succinic acid cocrystal with a known crystal structure[41], further referred to as polymorph I, formed initially at 124 °C but underwent a phase transition to form a new polymorph (form II) when kept at this temperature for >3 h. PXRD patterns showing the conversion of the physical mixture of isoniazid and succinic acid to cocrystal and the following polymorphic transition are presented in Figure 4.

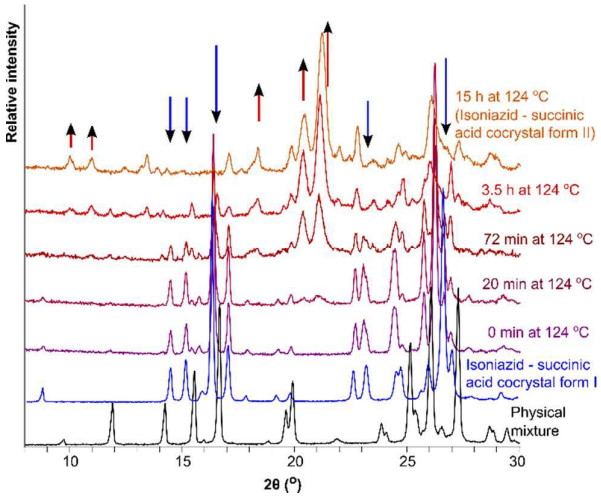


**Fig. 4** Powder X-ray diffraction patterns showing isoniazid–succinic acid cocrystal polymorph transition at 124 °C. Blue arrows indicate the disappearance of diffraction peaks characteristic to isoniazid–succinic acid cocrystal form I and the red arrows indicate the appearance of diffraction peaks characteristic to isoniazid–succinic acid cocrystal form II.

The thermal cocrystallisation of isoniazid and adipic acid returned the polymorph II. The thermal cocrystallisation in the mixture of isoniazid and sebacic acid was slow and only partial conversion was observed after 6 h of storage at 113 °C.

**Solvent vapour-assisted cocrystallisation**

In the previous examples, cocrystal formation was achieved by applying mechanical or thermal energy to the mixture of cocrystal ingredients; however, spontaneous cocrystallisation can also take place under favourable conditions. According to previous observations[62,63], such "favourable conditions" include humidity or the presence of solvent vapour. We found vapour-assisted cocrystallisation to be an easy method for preparation of pure isoniazid–dicarboxylic acid cocrystals. However, the time required for cocrystallisation depended on the length of the dicarboxylic acid. To assess the effect of solvent choice and acid molecule length, we have performed cocrystallisation experiments in the presence of water, ethanol, acetonitrile, ethyl acetate, chloroform and toluene as representatives of polar protic, polar aprotic and non-polar solvents. The availability of solubility data for pure dicarboxylic acids in these solvents was also considered as the solubility of compounds can influence the formation of cocrystals.

The physical mixtures of isoniazid and dicarboxylic acids were stored in the presence of solvent vapour for 4 h, then subjected to PXRD analysis (Figures S24-S31 in ESI). Following analysis, samples were exposed to solvent vapour for another 20 h and analysed using PXRD (Figures S24-S31 in ESI). Results of the quantitative analysis of these samples are shown in Figure 5 and in Figure 6. Rates of vapour-assisted cocrystallisation reactions show similar trends to those of mechanochemical cocrystallisation, with the formation of odd-chain acid cocrystals being faster than that of even-chain acid cocrystals. The reason for the alternation between reaction rates is likely related to aforementioned stability differences between odd-chain and even-chain diacid crystal lattices. These differences result in alternating trends in the saturated vapour pressure[37–40] and sublimation enthalpy[37] of the acids. As the sublimation is easier and the saturated vapour pressure is higher for odd-chain acids, the cocrystallisation of these acids to isoniazid proceeds faster. Furthermore, sublimation may increase the disorder in the surface layer[64] of crystallites, thus raising their reactivity.

For the longer dicarboxylic acids (suberic acid, azelaic acid and sebacic acid) cocrystallisation within the experimental time frame (24 h) was not observed. An exception was the isoniazid–suberic acid cocrystal that formed only in the presence of ethanol vapour. This exception is explained by adsorption of ethanol onto the surface of the sample, resulting in the formation of a liquid layer. It is thought that crystallisation of a cocrystal from this saturated solution had taken place. Since the experimental time frame of 24 h in the presence of water, acetonitrile, ethyl acetate, chloroform and toluene vapour was not sufficient to obtain cocrystals of long acids, we extended the time to 1 month. The prolonged experiment afforded the formation of isoniazid–suberic acid cocrystal in the presence of acetonitrile and ethyl acetate vapour. Neither isoniazid–azelaic acid nor isoniazid–sebacic acid cocrystal were obtained in vapochemical cocrystallisation experiments.

The effect of the solvent vapour can be explained by its adsorption on the surface of the sample followed by interaction with molecules in the surface layer of crystallites. Such interactions can be specific hydrogen bonds, π-π interactions, Van der Waals forces etc. and they depend on the molecular features of the solid and the solvent. The formation of new interactions between the molecules of the solid and those of the solvent can lead either to partial dissolution of crystallites or at least to increased plasticity of the surface. Both situations would favour the formation of new structures.

Figure 6 compares the influence of the solvent on the cocrystal formation process in solvent-assisted cocrystallisation experiments. From the data presented in Figure 6, it is obvious that isoniazid–malonic acid cocrystal and isoniazid–glutaric acid cocrystal in the presence of water vapour forms considerably faster than other cocrystals. This observation can be explained by the exceptionally good water solubility of malonic and glutaric acids, compared with other dicarboxylic acids, implying that good compound solubility can considerably facilitate vapochemical cocrystallisation. However, vapour-assisted cocrystallisation is possible even if the solubility of both compounds is poor. For example, isoniazid–dicarboxylic acid cocrystal formation took place in the presence of chloroform and toluene vapour, regardless of the low solubility of the compounds in these solvents. Generally, the cocrystallisation rate in the presence of organic solvent vapour follows the order ethanol > ethyl acetate ≈ acetonitrile > chloroform > toluene for all dicarboxylic acids. To relate the rate of cocrystal formation to properties of these solvents, we compared a set of solvent molecular descriptors[65,66], such as polarity, dipole moment, dielectric constant, H-bonding parameters etc. (Table S1 in ESI). This

comparison showed that the reaction rate rises with increasing hydrogen acceptor propensity[65–67] implying that the ability of the solvent to form H-bonds can greatly facilitate cocrystallisation.

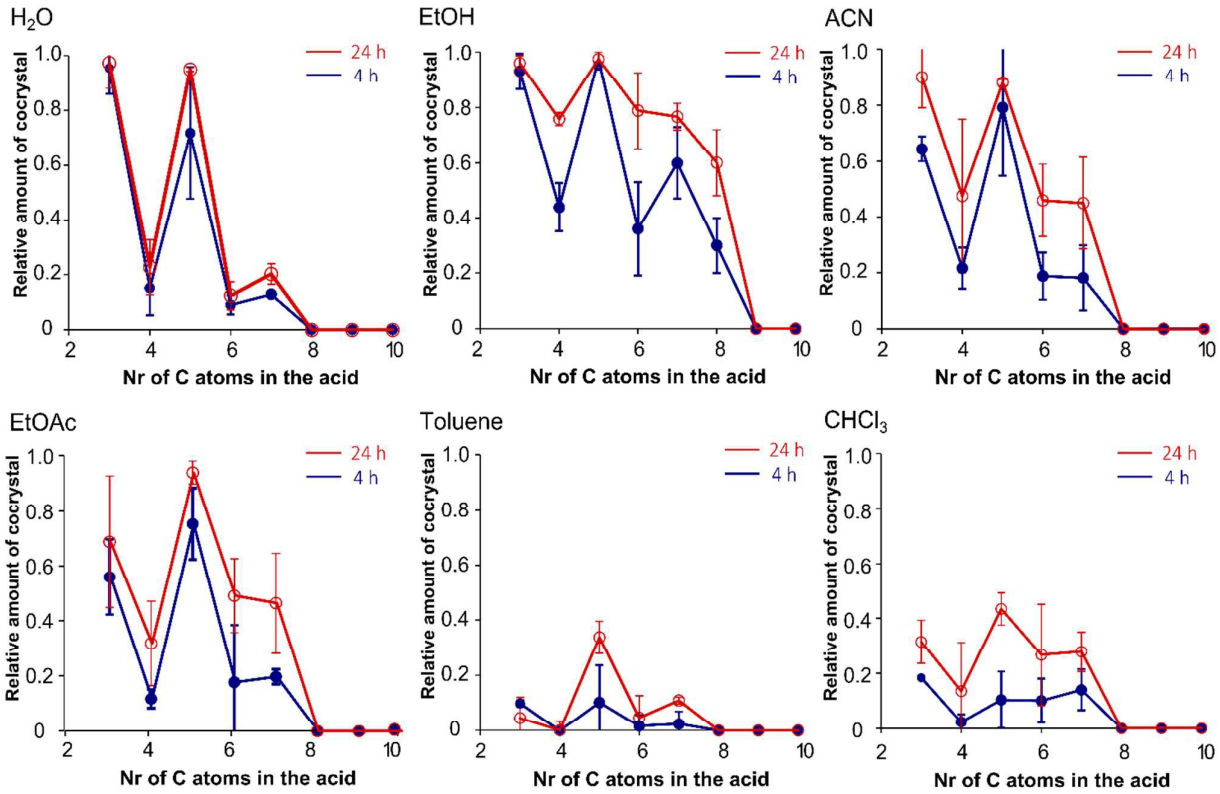


**Fig. 5** The amount of the cocrystal in physical mixtures of isoniazid and dicarboxylic acid as a function of acid chain length after storage for 4 and 24 h in the presence of water, ethanol, acetonitrile, ethyl acetate, chloroform and toluene vapour.

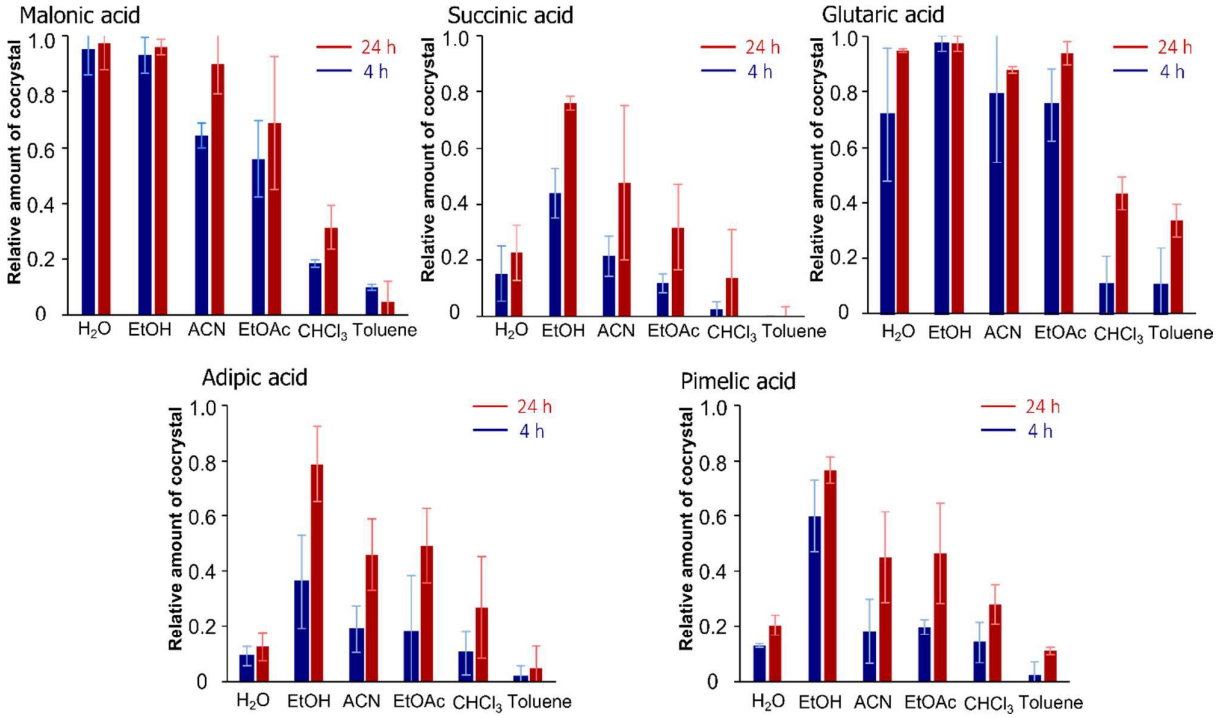


**Fig. 6** The amount of the isoniazid cocrystal with malonic, succinic, glutaric, adipic and pimelic acid in their physical mixtures, depending on the solvent choice.

The carboxyl groups of acids are good hydrogen donors and therefore, interactions with hydrogen acceptors are likely. However, the carbonyl oxygen can also act as a hydrogen acceptor, making interactions with hydrogen donor compounds possible. This is exemplified by the isoniazid–malonic acid cocrystal, which forms spontaneously, even under ambient conditions (50% RH, 22 °C). Malonic acid has a dense hydrogen bonding network, and the p$K_a$ values for both carboxylic groups differ more than those of other diacids[68]. Consequently, good hydrogen bond donors and acceptors easily interact with malonic acid molecules resulting in a strong accelerating effect on the reaction.

**Summary of cocrystallisation results**

To summarize all results obtained in this work, isoniazid–dicarboxylic acid ($C_3$–$C_8$ and $C_{10}$) cocrystals could be obtained using mechanochemical, thermal and vapochemical methods. Isoniazid–azelaic acid cocrystal, however, could not be obtained by any of these methods. Vapochemical method failed to provide the formation of the isoniazid–sebacic acid ($C_{10}$) cocrystal while mechanochemical and thermal methods allowed obtaining this cocrystal. An overview of the isoniazid–dicarboxylic acid cocrystallisation results (whether the cocrystal was obtained by the chosen method) is presented in Table 1. The choice of solvent significantly affects the outcome of vapochemical cocrystallisation; therefore, various solvents should be tested in order to identify the most appropriate for the system of interest.

**Table 1.**

The outcome of isoniazid and dicarboxylic acid cocrystallisation experiments using mechanochemical, thermal and vapochemical methods (*√* - formation of cocrystal was observed).

| Acid | Mechanochemical method | Thermal method | Vapochemical method |
|---|---|---|---|
| Malonic | √ | √ | √ |
| Succinic | √ | √ | √ |
| Glutaric | √ | √ | √ |
| Adipic | √ | √ | √ |
| Pimelic | √ | √ | √ |
| Suberic | √ | √ | √ |
| Azelaic | – | – | – |
| Sebacic | √ | √ | – |

**Crystal structure of isoniazid–adipic acid cocrystal polymorph II**

The crystal structure of isoniazid–adipic acid cocrystal prepared by crystallisation from methanol has been reported in the literature[41]. Our mechanochemical and thermochemical experiments returned a new polymorph (II) of this cocrystal. The crystal structure of the isoniazid–adipic acid cocrystal polymorph II was solved from powder X-ray diffraction data. Similarly to the known polymorph I[41], the polymorph II crystallizes in the monoclinic $P2_1/c$ space group with a molecule of isoniazid and half a molecule of adipic acid in the asymmetric unit. The relevant crystallographic data are available in Table S2 in ESI. The adipic acid molecule is located on the symmetry centre. Each carboxyl group of the acid forms two hydrogen bonds with two distinct isoniazid molecules (Figure 7). The hydroxyl oxygen of the carboxyl group acts as a proton donor to form an O–H···N hydrogen bond to pyridine N of isoniazid. The carbonyl oxygen, however, is a hydrogen acceptor in a N–H···O hydrogen bond with the isoniazid hydrazide group. In addition, two adjacent isoniazid molecules form a N–H···O hydrogen bond between their hydrazide groups.

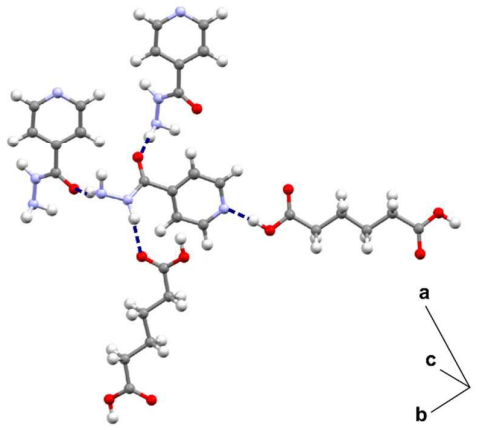


**Fig. 7** Hydrogen bonds in the isoniazid–adipic acid cocrystal polymorph II crystal structure.

Interestingly, the characteristic ring synthons $R_2^2(7)$ (between the isoniazid pyridine ring and carboxyl group) and $R_2^2(10)$ (between hydrazide groups of the isoniazid moieties) common to isoniazid–dicarboxylic acid cocrystals are not present in this crystal structure.

## Conclusions

Cocrystallisation of isoniazid to dicarboxylic acids ($C_3$–$C_{10}$) was conducted using three different cocrystallisation methods: mechanochemical, thermochemical and vapochemical. A comparison of the cocrystallisation results revealed that all three cocrystallisation methods can be used to produce isoniazid–dicarboxylic acid cocrystals. However, the efficiency of vapochemical and mechanochemical methods depends on the length of the dicarboxylic acid.

Generally, in mechanochemical and vapochemical reactions shorter dicarboxylic acids tend to form cocrystals considerably faster than longer ones, partially due to the higher mobility of small molecules. In all cases cocrystallisation is facilitated by conditions that promote molecular diffusion (humidity and elevated temperature).

The rate of cocrystallisation process was found to show the odd-even alternation effect in mechanochemical and vapochemical reactions. Cocrystallisation occurred more

rapidly to odd-chain than to even-chain dicarboxylic acids as a result of faster decomposition of the less stable odd-chain acid crystal structures. Vapour-assisted cocrystal formation with dicarboxylic acids was found to rely largely on the hydrogen-donor and hydrogen-acceptor properties of the solvent. Good proton acceptors offered advantage over other solvents. For preparation of pure cocrystal it is important to optimize the crystallisation conditions, such as milling time in mechanochemistry and solvent choice in vapochemistry. Poor choice of these parameters can result in failure of the method to provide the desired product.

The presence of the odd-even effect implies that the properties of compounds can significantly influence the rate of cocrystal formation. These results show that vapochemical method is promising for cocrystallisation of small organic molecules and could be used as an alternative method for cocrystal screening.

## Experimental

### Materials

Isoniazid and dicarboxylic acids were procured from commercial suppliers. Prior to cocrystallisation experiments, 5 g of each material were milled in the Retsch MM301 ball mill (10 mL stainless steel jar with one 1 cm stainless steel ball in each) for 10 minutes to reduce the particle size. Milled samples were kept under ambient conditions for one week and then sieved to obtain the 75 to 150 μm fraction.

### Cocrystallisation methods

**Thermal cocrystallisation.** Thermal cocrystallisation was performed using differential thermal analysis (DTA). Stoichiometric amounts of isoniazid and dicarboxylic acid were weighted with a precision of 0.1 mg and gently blended together in an agate mortar. This mixture (6–8 mg) was then transferred to an aluminium pan. DTA was performed using the Seiko Exstar6000 TG/DTA6300 (Seiko Instruments Inc., Japan). Physical mixtures were heated in open aluminium pans at a rate of 5 °C $min^{-1}$ in a nitrogen flow.

**Mechanochemical cocrystallisation.** Samples for mechanochemical cocrystallisation were prepared by weighting stoichiometric amounts of isoniazid and dicarboxylic acid so that the final mass of the sample was 0.3774 grams. Compounds were gently blended together in an agate mortar and placed in 5 mL milling jars containing two 8 mm and three 6 mm stainless steel balls in each jar (two different milling ball sizes were found to offer better data reproducibility). Samples were ground under ambient conditions (45%–55% relative humidity (RH) and 20–22 °C) for 5 and 15 minutes at a frequency of 20 Hz. Each milling experiment was performed in 3 replicates. The milling product was analysed by PXRD immediately after the experiment.

**Vapour-assisted cocrystallisation.** Physical mixtures for vapour-assisted cocrystallisation experiments were prepared by gently blending together stoichiometric amounts of isoniazid and dicarboxylic acid. The mixture (*ca*. 100 mg) was spread in a thin layer on the bottom of a glass vial and the vial was then placed in a desiccator containing the vapour of water, ethanol, acetonitrile, ethyl acetate, chloroform or toluene. After 4 h of storage, PXRD patterns were recorded for the samples. Then these samples were replaced in desiccators containing solvent vapour and kept for another 20 h. After this storage period PXRD patterns were again recorded for the samples. Three replicates were prepared for each sample and used to calculate the average composition. Samples were not ground before PXRD measurements, as grinding can facilitate cocrystallisation. The isoniazid–malonic acid cocrystal was found to form spontaneously, even under laboratory conditions (50% RH, 22 °C) and the isoniazid–malonic acid samples were covered with a polyethylene film during PXRD analysis to prevent the effect of moisture.

### PXRD analysis

PXRD analysis was performed using a Bruker AXS D8 Advance powder diffractometer (Bruker AXS GmbH, Germany) equipped with a LynxEye position sensitive detector and Cu Kα radiation (λ=1.5418 Å), 40 kV, 40 mA. Data were collected at ambient temperature with a step of 0.02° and scan speed of 0.1 s/step. VT-PXRD experiments to study thermal cocrystallisation of isoniazid and dicarboxylic acids were performed using a Bruker AXS D8 Discover powder diffractometer (Bruker AXS GmbH, Germany) equipped with an MRI temperature chamber. Copper Kα radiation (λ=1.5418 Å) was used in the experiments. Diffraction patterns were recorded with a 0.02° step size and a scan speed of 0.2 s per step in the 2θ range of 3 to 35°.

### Quantitative analysis using Rietveld method

Quantitative Rietveld analyses[69,70] of the X-ray diffraction data were performed using the Bruker Topas 4.2 software[71] with the fundamental parameters (FP) approach. The crystal structures of isoniazid[72] (CSD refcode INICAC01), malonic acid (CSD refcode MALNAC), succinic acid (CSD refcode SUCACB02), glutaric acid (CSD refcode GLURAC), adipic acid (CSD refcode ADIPAC), pimelic acid (CSD refcode PIMELA03), suberic acid (CSD refcode SUBRAC01), sebacic acid (CSD refcode SEBAAC), isoniazid–malonic acid cocrystal (FADGEY), isoniazid–succinic acid cocrystal (FADGIC), isoniazid–glutaric acid cocrystal (FADGOI), isoniazid–adipic acid cocrystal (FADGUO), isoniazid–pimelic acid cocrystal (FADHAV), isoniazid–sebacic acid cocrystal (SETROA) were obtained from the Cambridge Structural Database (CSD)[73] and used in the calculations. The crystal structure of the isoniazid–suberic acid cocrystal was determined by us from single crystal X-ray diffraction data[42]. The cell parameters of each structure before quantitative analysis were refined to PXRD data recorded on the D8 Advance diffractometer to compensate for the temperature difference during structure determination and PXRD experiments. The background of the powder patterns was described by a 2nd order Chebyschev polynomial. The unidentified phases in samples containing malonic and glutaric

acid were included in the refinement as peak phases. The results obtained were corrected for absorption and sample displacement. The preferred orientation was included in the refinement.

**Structure Determination from Powder X-ray Diffraction Data**

For structure determination PXRD patterns were recorded on a Bruker D8 Discover diffractometer using copper radiation (Cu Kα λ = 1.54180 Å) in transmission mode and a LynxEye (1D) detector. The tube was employed with voltage and current settings of 40 kV and 40 mA. The sample was loaded into a special glass Nr. 10 capillary (0.5 mm diameter). A capillary spinner (60 rpm) was used to minimize instrumental and sample packing aberrations. Upper knife edge was used to reduce the background produced by air scattering and lower knife edge was used to block the primary beam. The incident beam path of the diffractometer was equipped with a Göbel mirror, Soller slits, and a 0.6 mm divergence slit, while the diffracted beam path was equipped only with Soller slits. The diffraction patterns were recorded in a 2θ range of 4.5 to 70° at a 0.01° step size with a scan speed of 36 s per step.

Indexing, space group determination, structure solution and Rietveld refinement were conducted using EXPO2014[74]. The unit cell dimensions was determined by the N-TREOR09[75] indexing procedure with a set of 20–25 reflections found in 4.5°–40° 2θ range. Space group determination was carried out using a statistical assessment of systematic absences, and *Z*′ was determined based on density considerations. The space group was assigned as $P2_1/c$ with $Z'=1$. The cell and diffraction pattern profile parameters were refined according to the LeBail algorithm[76]. The background was modelled by a 20$^{th}$-order polynomial function of the Chebyschev type; peak profiles were described by the Pearson VII function.

The initial geometry of molecules was taken from the crystal structure of isoniazid–aipic acid cocrystal polymorph I[41]. The simulating annealing technique with dynamical occupancy correction was used to constantly adjust the conformation, position, and orientation of the trial model in the unit cell in order to maximize the agreement between calculated and measured diffraction data. The Rietveld refinement was carried out using soft constraints on bond distances and angles; In the Rietveld refinement, profile and cell parameters, isotropic thermal vibration, and preferred orientation parameters[77] were optimized to get an optimum crystal structure. The planar pyridine ring was treated as a rigid body, and soft constraints on bond distances and angles were used. The $U_{iso}$ values of the H atoms were constrained to be $1.2U_{iso}$ of those of the non-H atoms. The final Rietveld refinement showed a good agreement between the observed and calculated profiles (Figure 8).

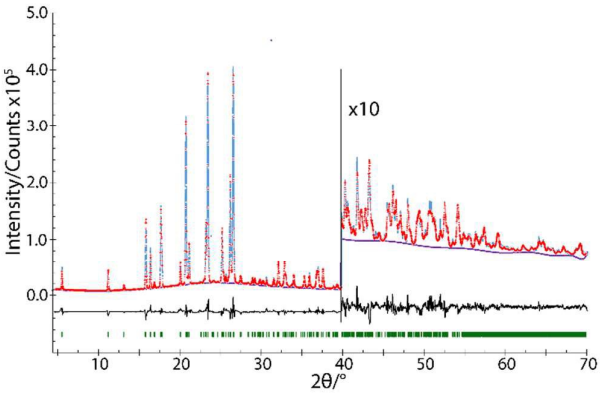


**Fig. 8** Final Rietveld fit for isoniazid–adipic acid cocrystal form II: red crosses – measured data points; blue line – calculated profile; black line – difference curve; green tick marks – calculated peak positions; violet line – background.

**Geometry optimization.** Geometry of the isoniazid–adipic acid cocrystal form II crystal structure was optimized using the DFT (Density-Functional Theory) PWscf (Plane-Wave Self-Consistent Field) package within Quantum ESPRESSO[78]. Calculations were performed with the PBE[79] exchange correlation functional, and ultra-soft pseudopotentials with a wave function cut-off of 44 Ry and a secondary cut-off of 176 Ry. Pseudopotentials C.pbe-rrkjus.UPF, F.pbe-n van.UPF, N.pbe-rrkjus.UPF, O.pbe-rrkjus.UPF and H.pbe-rrkjus.UPF were acquired from the Quantum ESPRESSO pseudopotential data base[80]. Pseudopotentials, energy and force thresholds for structural relaxation were used as described elsewhere[81]. A k-point grid of 2 x 2 x 2 was used.

## Notes and references


1 J. W. Steed, *Trends Pharmacol. Sci.*, 2013, **34**, 185–93.
2 T. Friščić and W. Jones, *J. Pharm. Pharmacol.*, 2010, **62**, 1547–59.
3 N. Qiao, M. Li, W. Schlindwein, N. Malek, A. Davies and G. Trappitt, *Int. J. Pharm.*, 2011, **419**, 1–11.
4 D. Braga, F. Grepioni, G. I. Lampronti, L. Maini and A. Turrina, *Cryst. Growth Des.*, 2011, **11**, 5621–5627.
5 N. Schultheiss and A. Newman, *Cryst. Growth Des.*, 2009, **9**, 2950 – 2967.
6 S. Vijayalakshmi and S. Kalyanaraman, *Spectrochim. Acta. A. Mol. Biomol. Spectrosc.*, 2014, **120**, 14–8.
7 E. D. D'Silva, G. K. Podagatlapalli, S. V. Rao, D. N. Rao and S. M. Dharmaprakash, *Cryst. Growth Des.*, 2011, **11**, 5362–5369.
8 H. T. Black and D. F. Perepichka, *Angew. Chemie - Int. Ed.*, 2014, **53**, 2138–2142.
9 A. G. Zalte and R. B. Saudagar, *Int. J. Sci. Prog. Res.*, 2015, **12**, 32–35.
10 E. Gagniere, D. Mangin, F. Puel, J. P. Valour, J. P. Klein and O. Monnier, *J. Cryst. Growth*, 2011, **316**, 118–125.
11 K. Fucke, S. A. Myz, T. P. Shakhtshneider, E. V. Boldyreva and U. J. Griesser, *New J. Chem.*, 2012, **36**, 1969–1977.
12 T. Leyssens, N. Tumanova, K. Robeyns, N. Candoni and S. Veesler, *CrystEngComm*, 2014, **16**, 9603–9611.
13 E. Lu, N. Rodríguez-Hornedo and R. Suryanarayanan,

*CrystEngComm*, 2008, **10**, 665–668.
14 A. N. Manin, A. P. Voronin, K. V. Drozd, N. G. Manin, A. Bauer-brandl and G. L. Perlovich, *Eur. J. Pharm. Sci.*, 2014, **65**, 56–64.
15 T. Friščić, S. L. Childs, S. A. A. Rizvi and W. Jones, *CrystEngComm*, 2009, **11**, 388–403.
16 S. L. James, C. J. Adams, C. Bolm, D. Braga, P. Collier, T. Friščić, F. Grepioni, K. D. M. Harris, G. Hyett, W. Jones, A. Krebs, J. Mack, L. Maini, A. G. Orpen, I. P. Parkin, W. C. Shearouse, J. W. Steed and D. C. Waddell, *Chem. Soc. Rev.*, 2012, **41**, 413–447.
17 T. Friščić, *J. Mater. Chem.*, 2010, **20**, 7599–7605.
18 N. Shan, F. Toda and W. Jones, *Chem. Commun.*, 2002, 2372–2373.
19 S. Karki, T. Friščić and W. Jones, *CrystEngComm*, 2009, **11**, 470–481.
20 A. V. Trask, W. D. S. Motherwell and W. Jones, *Chem. Commun.*, 2004, 890–891.
21 A. V Trask, N. Shan, W. D. S. Motherwell, W. Jones, S. Feng, R. B. H. Tan and K. J. Carpenter, *Chem. Commun.*, 2005, 880–882.
22 H. Yamashita, Y. Hirakura, M. Yuda, T. Teramura and K. Terada, *Pharm. Res.*, 2013, **1**, 70–80.
23 C. Maheshwari, A. Jayasankar, N. A. Khan, G. E. Amidon and N. Rodríguez-Hornedo, *CrystEngComm*, 2009, **11**, 493–500.
24 K. K. Arora, N. G. Tayade and R. Suryanarayanan, *Mol. Pharm.*, 2011, **8**, 982–989.
25 A. Jayasankar, D. J. Good and N. Rodríguez-Hornedo, *Mol. Pharm.*, 2007, **4**, 360–372.
26 D. Braga, S. L. Giaffreda, F. Grepioni, M. R. Chierotti, R. Gobetto, G. Palladino and M. Polito, *CrystEngComm*, 2007, **9**, 879–881.
27 D. Braga, G. Palladino, M. Polito, K. Rubini, F. Grepioni, M. R. Chierotti and R. Gobetto, *Chem. - A Eur. J.*, 2008, **14**, 10149–10159.
28 A. Jayasankar, A. Somwangthanaroj, Z. J. Shao and N. Rodríguez-Hornedo, *Pharm. Res.*, 2006, **23**, 2381–2392.
29 R. Bobrovs, L. Seton and N. Dempster, *CrystEngComm*, 2015, **17**, 5237–5251.
30 L. J. Thompson, R. S. Voguri, L. Male and M. Tremayne, *CrystEngComm*, 2011, **13**, 4188–4195.
31 C. B. Aakeröy, S. Forbes and J. Desper, *J. Am. Chem. Soc.*, 2009, **131**, 17048–17049.
32 D. Braga, E. Dichiarante, G. Palladino, F. Grepioni, M. R. Chierotti, R. Gobetto and L. Pellegrino, *CrystEngComm*, 2010, **12**, 3534 – 3536.
33 P. Vishweshwar, A. Nangia and V. M. Lynch, *Cryst. Growth Des.*, 2003, **3**, 783 – 790.
34 V. R. Thalladi, M. Nüsse and R. Boese, *J. Am. Chem. Soc.*, 2000, **122**, 9227–9236.
35 H. Zhang, Q. Yin, Z. Liu, J. Gong, Y. Bao, M. Zhang, H. Hao, B. Hou and C. Xie, *J. Chem. Thermodyn.*, 2014, **77**, 91–97.
36 H. Zhang, C. Xie, Z. Liu, J. Gong, Y. Bao, M. Zhang, H. Hao, B. Hou and Q. Yin, *Ind. Eng. Chem. Res.*, 2013, **52**, 18458–18465.
37 M. Bilde, B. Svenningsson, J. Mønster and T. Rosenørn, *Environ. Sci. Technol.*, 2003, **37**, 1371–1378.
38 E. A. Bruns, J. Greaves and B. J. Finlayson-Pitts, *J. Phys. Chem. A*, 2012, **116**, 5900–5909.
39 C. D. Cappa, E. R. Lovejoy and A. R. Ravishankara, *J. Phys. Chem. A*, 2007, **111**, 3099–3109.
40 M. Bilde, K. Barsanti, M. Booth, C. D. Cappa, N. M. Donahue, E. U. Emanuelsson, G. McFiggans, U. K. Krieger, C. Marcolli, D. Topping, P. Ziemann, M. Barley, S. Clegg, B. Dennis-Smither, M. Hallquist, Å. M. Hallquist, A. Khlystov, M. Kulmala, D. Mogensen, C. J. Percival, F. Pope, J. P. Reid, M. a. V. Ribeiro da Silva, T. Rosenoern, K. Salo, V. P. Soonsin, T. Yli-Juuti, N. L. Prisle, J. Pagels, J. Rarey, A. a. Zardini and I. Riipinen, *Chem. Rev.*, 2015, **115**, 4115–4156.
41 A. Lemmerer, J. Bernstein and V. Kahlenberg, *CrystEngComm*, 2010, **12**, 2856–2864.
42 I. Sarcevica, L. Orola, M. V Veidis, A. Podjava and S. Belyakov, *Cryst. Growth Des.*, 2013, **13**, 1082–1090.
43 R. Kaur, S. S. R. R. Perumal, A. J. Bhattacharyya, S. Yashonath and T. N. Guru Row, *Cryst. Growth Des.*, 2014, **14**, 423–426.
44 T. J. Chiya and A. Lemmerer, *CrystEngComm*, 2012, **14**, 5124–5127.
45 S. Aitipamula, A. B. H. Wong, P. S. Chow and R. B. H. Tan, *CrystEngComm*, 2013, **15**, 5877–5887.
46 S. M. A. Mashhadi, U. Yunus, M. H. Bhatti and M. N. Tahir, *J. Mol. Struct.*, 2014, **1076**, 446–452.
47 N. Ravikumar, G. Gaddamanugu and K. Anand Solomon, *J. Mol. Struct.*, 2013, **1033**, 273–279.
48 I. Sarcevica, L. Orola, M. V Veidis and S. Belyakov, *Acta Crystallogr. Sect. C, Struct. Chem.*, 2014, **70**, 392–395.
49 B. Swapna, D. Maddileti and A. Nangia, *Cryst. Growth Des.*, 2014, **14**, 5991–6005.
50 A. Lemmerer, J. Bernstein and V. Kahlenberg, *CrystEngComm*, 2011, **13**, 5692–5708.
51 M. Sevukarajan, R. Sodanapalli, B. Thanuja and R. Nair, *J. Biomed. Sci.*, 2011, **3**, 397–402.
52 P. Grobely, A. Mukherjee and G. R. Desiraju, *CrystEngComm*, 2011, **13**, 4358–4364.
53 A. Lemmerer, *CrystEngComm*, 2012, **14**, 2465–2478.
54 Z.-J. Jiang, L. Lu-De, X.-D. Wu and X.-J. Yang, *Chinese J. Inorg. Chem.*, 2009, **25**, 746–750.
55 M. C. R. Freitas, J. M. S. António, R. L. Ziolli, M. I. Yoshida, N. A. Rey and R. Diniz, *Polyhedron*, 2011, **30**, 1922–1926.
56 J. C. Hanson, N. Camerman and A. Camerman, *J. Med. Chem.*, 1981, **24**, 1369–71.
57 G. G. Tsintsadze, G.V. Dzhavakhishvili, Z.O. Aleksandrov, Y. T. Struchkov and A. P. Narimanidze, *Russ. J. Coord. Chem.*, 1980, **6**, 785.
58 L. B. Zinner, D. E. Crotty, T. J. Anderson and M. D. Glick, *Inorg. Chem.*, 1979, **18**, 2045–2048.
59 L. BenHamada and A. Jouini, *Mater. Res. Bull.*, 2006, **41**, 1917–1924.
60 V. O. Gel'mbol'dt, V. N. Davydov, L. V. Koroeva and E. V. Ganin, *Russ. J. Inorg. Chem.*, 2002, **47**, 987.
61 V. S. Mandala, S. J. Loewus and M. A. Mehta, *J. Phys. Chem. Lett.*, 2014, **5**, 3340–3344.
62 T. Ervasti, J. Aaltonen and J. Ketolainen, *Int. J. Pharm.*, 2015, **486**, 121–130.
63 I. Sarceviča, L. Orola, K. P. Nartowski, Y. Z. Khimyak, A. N. Round and L. Fábián, *Mol. Pharm.*, 2015, **12**, 2981–2992.
64 A. Newman and G. Zografi, *J. Pharm. Sci.*, 2014, **103**, 1–10.
65 C.-H. Gu, H. Li, R. B. Gandhi and K. Raghavan, *Int. J. Pharm.*, 2004, **283**, 117–25.
66 D. Xu and N. Redman-Furey, *Int. J. Pharm.*, 2007, **339**, 175–188.
67 C. A. Hunter, *Angew. Chemie - Int. Ed.*, 2004, **43**, 5310–5324.

68 C. Tong, M. Blanco, W. A. Goddard and J. H. Seinfeld, *Environ. Sci. Technol.*, 2004, **38**, 3941–3949.
69 H. M. Rietveld, *Aust. J. Phys.*, 1988, **41**, 113–116.
70 D. L. Bish and S. A. Howard, *J. Appl. Crystallogr.*, 1988, **21**, 86–91.
71 R. W. Cheary and A. Coelho, *J. Appl. Crystallogr.*, 1992, **25**, 109–121.
72 T. N. Bhat, T. P. Singh and M. Vijayan, *Acta Crystallogr. Sect. B Struct. Sci.*, 1974, **30**, 2921–2922.
73 F. H. Allen, *Acta Crystallogr. Sect. B Struct. Sci.*, 2002, **58**, 380–388.
74 A. Altomare, C. Cuocci, C. Giacovazzo, A. Moliterni, R. Rizzi, N. Corriero and A. Falcicchio, *J. Appl. Crystallogr.*, 2013, **46**, 1231–1235.
75 A. Altomare, G. Campi, C. Cuocci, L. Eriksson, C. Giacovazzo, A. Moliterni, R. Rizzi and P.-E. Werner, *J. Appl. Crystallogr.*, 2009, **42**, 768–775.
76 A. Le Bail, H. Duroy and J. L. Fourquet, *Mater. Res. Bull.*, 1988, **23**, 447–452.
77 W. A. Dollase, *J. Appl. Crystallogr.*, 1986, **19**, 267–272.
78 P. Giannozzi, S. Baroni, N. Bonini, M. Calandra, R. Car, C. Cavazzoni, D. Ceresoli, G. L. Chiarotti, M. Cococcioni, I. Dabo, A. Dal Corso, S. de Gironcoli, S. Fabris, G. Fratesi, R. Gebauer, U. Gerstmann, C. Gougoussis, A. Kokalj, M. Lazzeri, L. Martin-Samos, N. Marzari, F. Mauri, R. Mazzarello, S. Paolini, A. Pasquarello, L. Paulatto, C. Sbraccia, S. Scandolo, G. Sclauzero, A. P. Seitsonen, A. Smogunov, P. Umari and R. M. Wentzcovitch, *J. Phys. Condens. Matter*, 2009, **21**, 395502.
79 J. P. Perdew, K. Burke and M. Ernzerhof, *Phys. Rev. Lett.*, 1996, **77**, 3865–3868.
80 *http://www.quantum-espresso.org/pseudopotentials*.
81 A. M. Lund, A. M. Orendt, G. I. Pagola, M. B. Ferraro and J. C. Facelli, *Cryst. Growth Des.*, 2013, **13**, 2181–2189.

**For Table of Contents only:**

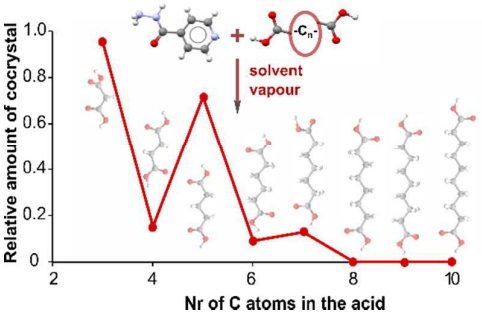


Systematic study on mechanochemical, thermal and vapochemical cocrystallisation demonstrates the effect of compound properties on the outcome of the reaction.